

Diffraction photoproduction of dijets at ZEUS

Roger Renner (on behalf of the ZEUS Collaboration)* and S. Kagawa†

**Physikalisches Institut, University of Bonn*

†*Department of Physics, University of Tokyo*

Abstract. The diffractive photoproduction of dijets has been studied using 77.6 pb^{-1} of data taken by the ZEUS detector at HERA. The measurements have been made in the kinematic range $0.2 < y < 0.85$ and $x_P < 0.035$, where y is the inelasticity and x_P is the fraction of the proton momentum taken by the diffractive exchange. The jets are reconstructed using the k_T algorithm. The two highest transverse energy jets are required to satisfy $E_T > 7.5$ and 6.5 GeV, respectively, and to lie in the pseudorapidity range $-1.5 < \eta < 1.5$. Differential cross sections have been measured and are confronted with the predictions from leading order Monte Carlo models and next-to-leading order QCD calculations.

Keywords: diffractive photoproduction dijets ZEUS

PACS: 13.60.-r

INTRODUCTION

Diffractive dijets provide an important means to test whether factorisation holds in photoproduction (PHP) as it has been shown to hold in deep inelastic scattering (DIS) [1]. In PHP, the exchanged photon emitted from the incoming electron or positron¹ can either interact directly or as a source of quarks and gluons (resolved PHP). In the direct process, the photon is point-like and mimics the DIS process. In the resolved process, rescattering between the hadronic content of the photon and the proton may lead to a breakdown of factorisation, as was observed and discussed in [2, 3]. In one model, that takes rescattering into account, contributions from resolved PHP were predicted to be suppressed by a factor 0.34 [4].

In this presentation, data enriched in direct and resolved PHP are compared separately with leading order (LO) Monte Carlo as well as next-to-leading (NLO) QCD calculations to test for such factorisation breaking.

EXPERIMENTAL SET-UP

The analysis is based on data with an integrated luminosity of 77.6 pb^{-1} which was collected with the ZEUS detector [5] at the HERA collider in the years 1999/2000. The energies of the incoming protons and electrons were 920 GeV and 27.6 GeV, respectively. The jets are reconstructed using information from the central tracking detector and the compensating uranium-scintillator calorimeter. Diffractive dijet events are selected

¹ Hereafter, “electron” is used to refer to both electron and positron.

by requiring a rapidity gap between the direction of the incoming proton and the most-forward energy deposits² in the forward calorimeter (FCAL) or the forward plug calorimeter (FPC), which is located around the beampipe inside the FCAL, extending the coverage in pseudorapidity up to $\eta \simeq 5$.

KINEMATICS AND DATA SELECTION

Diffractive dijet events are described by the process $ep \rightarrow ep + X(\text{jet} + \text{jet} + X')$. In PHP both the scattered electron and the scattered proton escape down the beampipe and remain undetected. The hadronic system X with invariant mass M_X contains the dijet system and any other hadronic activity X' . The kinematic variables used in this analysis are depicted in Fig. 1 and are defined as follows:

- Q^2 , the photon virtuality;
- y , the energy fraction of the electron carried by the exchanged photon;
- x_γ , the longitudinal momentum fraction of the photon carried by the parton;
- x_{IP} , the longitudinal momentum fraction of the proton entering the diffractive exchange, also referred to as Pomeron(IP)-exchange;
- z_{IP} , the longitudinal momentum fraction of the diffractive exchange carried by the parton;
- $E_T^{jet\ 1,2}$ and $\eta^{jet\ 1,2}$, the transverse energy and pseudorapidity of the two jets with the highest E_T as reconstructed by the k_T algorithm [6] run in the longitudinally invariant inclusive mode in the laboratory frame [7].

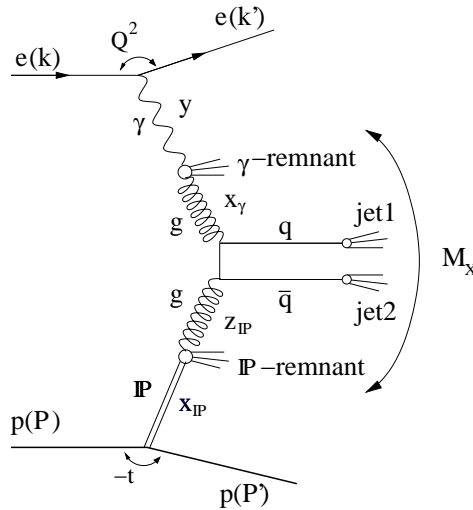


FIGURE 1. Depiction of the production of diffractive dijets in resolved PHP

² above noise threshold

For x_γ and z_{IP} , the observable estimators x_γ^{obs} and z_{IP}^{obs} are calculated as defined below:

$$x_\gamma^{obs} = \frac{\sum_{jet1,2} E_T^{jet} e^{-\eta^{jet}}}{2yE_e} \quad z_{IP}^{obs} = \frac{\sum_{jet1,2} E_T^{jet} e^{\eta^{jet}}}{2x_{IP}E_p}$$

The observable x_γ^{obs} is an estimator of the photon momentum fraction entering the dijet system. The range $x_\gamma^{obs} > 0.75$ ($x_\gamma^{obs} \leq 0.75$) is chosen to select data enriched with direct (resolved) PHP events [8]. The observable z_{IP}^{obs} is sensitive to the parton densities in the diffractive exchange.

The cross sections are measured in the following kinematic region:

- $Q^2 < 1.0 \text{ GeV}^2$, $0.2 < y < 0.85$;
- $x_{IP} < 0.035$;
- $E_T^{jet1} > 7.5 \text{ GeV}$, $E_T^{jet2} > 6.5 \text{ GeV}$, $-1.5 < \eta^{jet1,2} < 1.5$

PHP events are selected by requiring that no scattered electron candidate is found in the detector. For diffractive events a rapidity gap covering the pseudorapidity range $3 < \eta < 5$ was required. Background from cosmic events was rejected by a cut based on the timing of the two jets with highest E_T . After applying all cuts, 10673 events remain. The background from events with an undetected low-mass dissociative proton system is estimated to be $(16 \pm 4)\%$ [9] and independent from the measured variables. This fraction is statistically subtracted from all cross sections. Background from non-diffractive events is expected to be less than 10% and is not subtracted.

THEORETICAL PREDICTIONS

The data are compared to LO(+shower) Monte Carlo and NLO QCD calculations at hadron level.

The LO Monte Carlo is generated with RAPGAP [10] using the photon structure function GRV-G-HO and H1-fit2 [11] for the diffractive PDFs. Subsequently, the parton shower model MEPS [12] and the hadronisation model JETSET [13, 14] are applied. The LO Monte Carlo sample is also used to correct the data to the hadron level to account for acceptance losses.

NLO calculations on hadron level were provided by M. Klasen and G. Kramer [15] and are compared to data in two different ways. In one model resolved PHP is suppressed by a factor of $R = 0.34$ as motivated by [4], whereas in the other model no suppression of resolved PHP is applied ($R = 1$). In both cases no suppression was applied on direct PHP. The NLO predictions use the preliminary H1-2002 fit [16] for the diffractive PDFs. The renormalisation and factorisation scales were varied from $\frac{1}{2}E_T^{jet1}$ to $2E_T^{jet1}$ to account for theoretical uncertainties [15]. LO Monte Carlo is used to correct the predictions from the parton level³ to the hadron level.

³ after parton showers

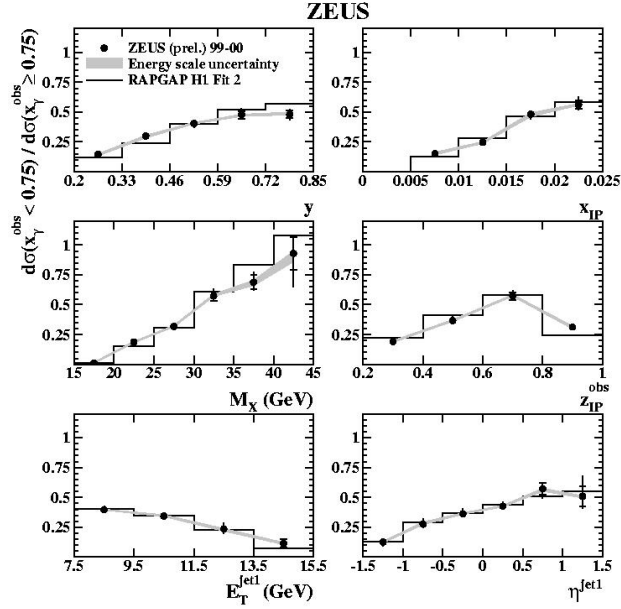


FIGURE 2. The ratio of single differential cross sections in y , x_P , M_X , z_P , E_T^{jet1} and η^{jet1} of data and LO Monte Carlo. The data are shown as dots, with the corresponding energy scale uncertainty shown as a band; the inner error bars indicate the statistical uncertainty and the outer error bars indicate the statistical and systematic uncertainties added in quadrature. The solid line show the prediction of the LO RAPGAP Monte Carlo. The H1 Fit2 diffractive PDFs are used.

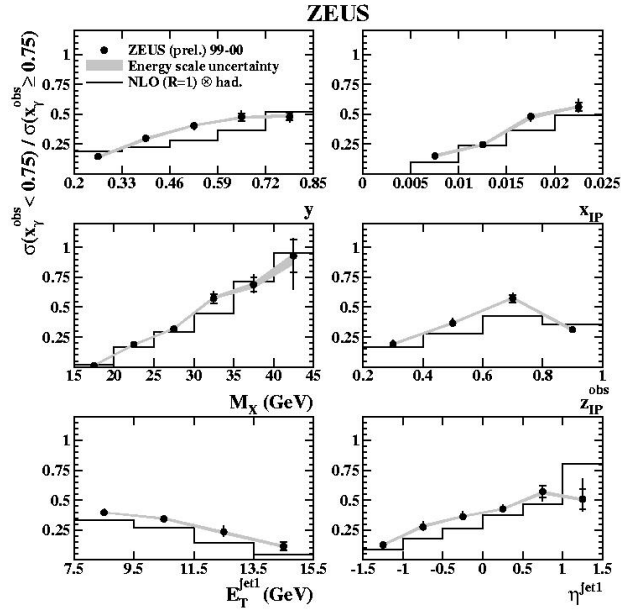


FIGURE 3. The ratio of single differential cross sections in y , x_P , M_X , z_P , E_T^{jet1} and η^{jet1} of data and NLO QCD calculations. For details of the data, see caption of Fig. 2. The solid line show the prediction of the NLO QCD calculation. The diffractive PDFs are from the H1 2002 fit.

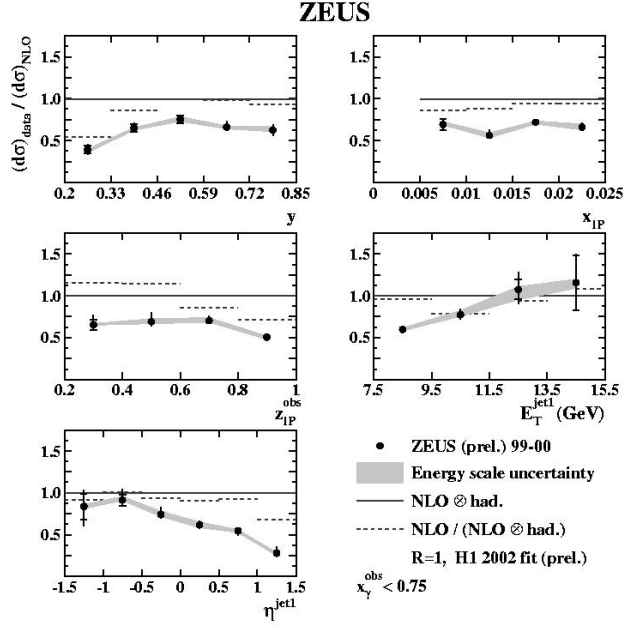


FIGURE 4. The ratio of data to the NLO QCD predictions of the single differential cross sections in y , x_P , M_X , z_P^{obs} , E_T^{jet1} and η^{jet1} for the sample enriched in resolved PHP ($x_\gamma^{obs} < 0.75$). For details of the data, see caption of Fig. 2. The solid lines indicate the expectations for $R = 1$. The dashed lines show the ratio of parton level to hadron level for NLO ($R = 1$). The diffractive PDFs are from the H1 2002 fit.

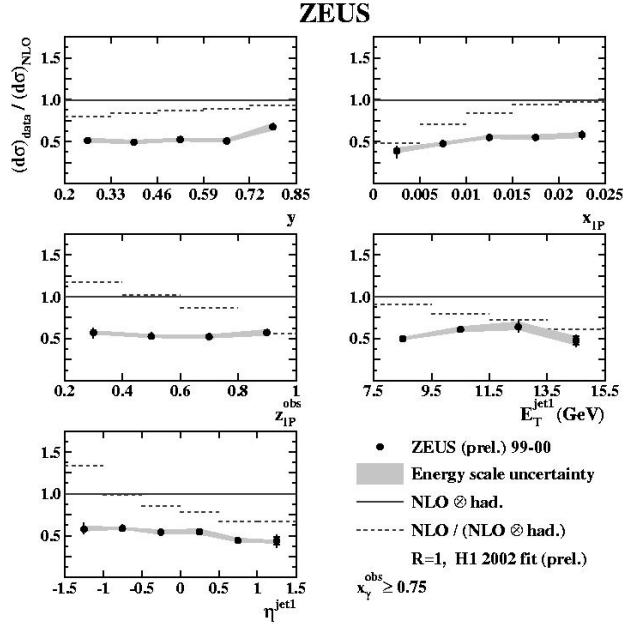


FIGURE 5. The ratio of data to the NLO QCD predictions of the single differential cross sections in y , x_P , M_X , z_P^{obs} , E_T^{jet1} and η^{jet1} for the sample enriched in direct PHP ($x_\gamma^{obs} \leq 0.75$). For details of the data, see caption of Fig. 2. For details of NLO predictions, see caption of Fig. 4.

RESULTS

The cross sections are measured as a function of y , x_P , M_X , x_γ^{obs} , z_{pP}^{obs} , E_T^{jet1} and η^{jet1} and presented separately for the samples enriched with direct and resolved PHP.

The LO Monte Carlo describes the data well as can be seen in Fig. 2, which shows the ratio of the direct vs. resolved enriched sample for both data and MC events and has the benefit that certain uncertainties, like the normalisation factor for MC, cancel out.

The ratio is also fairly well described by the NLO predictions (Fig. 3) of Klasen and Kramer. The ratio of data to NLO ($R = 1$) is shown separately for the resolved and direct enriched samples in Figs. 4 and 5. For resolved PHP ($x_\gamma^{obs} < 0.75$) the ratio is flat but data are lower by a factor of 2 compared to NLO. Deviations are seen at small E_T^{jet1} and high η^{jet1} , which are known to be sensitive to the structure function of the photon [17]. For direct PHP ($x_\gamma^{obs} \geq 0.75$) the ratio is also uniformly flat and data are also lower by a factor of 2. This is in contradiction to theoretical considerations which predict a suppression factor only for resolved PHP [4] and could indicate that a global suppression of both direct and resolved PHP is more likely. However, uncertainties in the diffractive PDFs need to be evaluated before stronger conclusions can be made.

REFERENCES

1. J.C. Collins, *Proof of factorisation for diffractive hard scattering*. Phys. Rev. **D 57**, 3051 (1998), hep-ph/9709499.
2. CDF Coll., T. Affolder et al., *Diffractive dijets with a leading antiproton in $p\bar{p}$ collisions at $\sqrt{s} = 1800$ GeV*. Phys. Rev. Lett. **84**, 5043 (2000).
3. A.B. Kaidalov, V.A. Khoze, A.D. Martin and M.G. Ryskin, *Probabilities of rapidity gaps in high energy interactions*. Eur. Phys. J. **C 21**, 521 (2001), hep-ph/0105145
4. A.B. Kaidalov, V.A. Khoze, A.D. Martin and M.G. Ryskin, Eur. Phys. J. **C21**, 521 (2003).
5. ZEUS Coll., U. Holm (ed.), *The ZEUS Detector*. Status Report (unpublished), DESY (1993), available on www-zeus.desy.de/bluebook/bluebook.html.
6. S. Catani et al., Nucl. Phys. **B 406**, 187 (1993).
7. S.D. Ellis and D.E. Soper, Phys. Rev. **D48**, 3160 (1993).
8. ZEUS Coll., S. Chekanov et al., Eur. Phys. J. **C23**, 615 (2001).
9. ZEUS Coll., S. Chekanov et al., Nucl. Phys. **B672**, 3 (2003).
10. H. Jung, *The RAPGAP Monte Carlo for Deep Inelastic Scattering version 2.08/00* (unpublished). 2001.
11. H1 Coll., C. Adloff et al., Z. Phys. **C 76**, 613 (1997).
12. R.K. Ellis, W.J. Stirling and B.R. Webber, *QCD and Collider Physics*, Cambridge Monographs on Particle Physics, Nuclear Physics and Cosmology, Vol.8.
13. M. Bengtsson and T. Sjöstrand, Comp. Phys. Comm. **46**, 43 (1987).
14. T. Sjöstrand, Comp. Phys. Comm. **82**, 74 (1994).
15. M. Klasen and G. Kramer, Preprint DESY-04-011 (hep-ph/0401202), 2004.
16. H1 Coll., *paper 980 submitted to 31. Intl. Conf. on High Energy Physics ICHEP 2002, Amsterdam, and paper 089 submitted to the EPS 2003 Conf., Aachen* (unpublished).
17. ZEUS Coll., S. Chekanov et al., Eur. Phys. J. **C 23**, 615 (2002).